Phase change characteristics of $Ge_1Cu_2Te_3$ films

Y. Sutou, Y. Saito, T. Kamada, M. Sumiya and J. Koike
Department of Materials Science, Graduate School of Engineering, Tohoku University,
6-6-11 Aoba-yama, Sendai 980-8579
ysutou@material.tohoku.ac.jp

ABSTRACT

The phase change behaviors of amorphous $Ge_1Cu_2Te_3$ (GCT) films prepared by sputter deposition were investigated by differential scanning calorimetric (DSC), two-point probe and atomic force microscopic measurements. It was found by the DSC measurement that the GCT film showed crystallization temperature of about 235°C at a heating rate of 10°C/min and melting point of about 510°C. The GCT memory device shows typical switching behaviors and exhibited a 10% lower power consumption for the reset operation than the GST memory device. The GCT amorphous film was found to show a thickness increase of only 2.0% with crystallization. Moreover, it was confirmed by isothermal annealing measurements that the GCT amorphous film shows a higher thermal stability than the GST amorphous film. Moreover, it was also demonstrated by the Ozawa method that the GCT amorphous film shows a high thermal stability and is estimated to show shows 10-year data lifetime at the maximum temperature of 135°C.

Key words: Ge-Cu-Te, crystallization behaviors, volume change, switching behaviors

1. INTRODUCTION

Te-based chalcogenide thin films have attracted attention as phase change materials (PCMs) for phase change random access memory (PCRAM). $Ge_2Sb_2Te_5$ (GST) is most widely studied compound for PCRAM application because it shows a fast crystallization [1,2]. The amorphous GST crystallizes first into a cubic state at around 150°C, and then into a more stable hexagonal state at around 350°C by further heating [1,3]. The crystallization mechanisms of GST amorphous film have been studied by isothermal and non-isothermal experiments [4-7]. However, GST has a low crystallization temperature T_x of about 150°C and a high melting point T_m of over 600°C [1,3]. A low T_x limits data retention capability and a high T_m causes high power consumption for reset operation. According to the International Technology Roadmap for Semiconductors (ITRS), the expected operating temperature for the PCRAM that guarantees a minimum operating data retention capability of 10 years is set to be 125°C beyond 2013 for high temperature operations, e.g., automotive applications. The GST has been reported to show a 10-year lifetime at the maximum temperature of 85 - 110°C [8-10], which is not satisfactory for high temperature applications.

Very recently, the present authors have found that a $Ge_1Cu_2Te_3$ (GCT) amorphous film has a high crystallization temperature of over 200˚C [11]. Figure 1 shows a pseudobinary phase diagram of Cu_2Te-$Ge_{33.3}Te_{66.7}$, which indicates

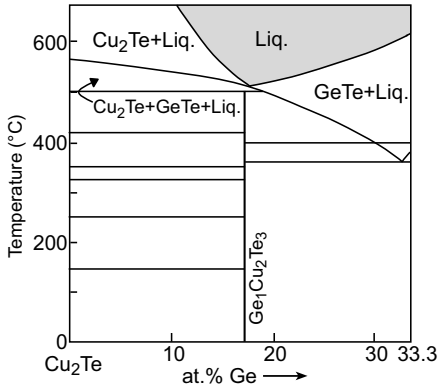

Figure 1 Cu_2Te-$Ge_{33.3}Te_{66.7}$ pseudobinary phase diagram [12]. $Ge_1Cu_2Te_3$ compound has a low melting temperature of about 500°C. Liq. : Liquid phase.

that the GCT compound has a low melting point of about 500˚C [12]. If the GCT shows reversible phase transition between amorphous and crystalline states, it can be used as a PCM. In this study, the memory switching behaviors of GCT film were investigated using simple memory devices. Moreover, the crystallization behaviors and thermal stability of amorphous GCT films were investigated by two-point probe, atomic force microscopic and differential scanning calorimetric measurements.

2. EXPERIMENTS

Phase change temperatures of $Ge_1Cu_2Te_3$ (GCT) film were investigated by differential scanning calorimetric (DSC) measurement. For the DSC measurement, GCT film was prepared as follows: (1) GCT film with a thickness of 1500 nm was deposited on photoresist substrate by sputtering of a GCT alloy target. (2) the photoresist substrate was dissolved in acetone. (3) Only the obtained GCT film was set into alumina pan for the DSC measurement. The DSC measurement was carried out at a heating rate of 10°C/min for crystallization and at a heating rate of 3°C/min for melting. Simple memory devices with GCT films as shown in Fig. 2 were fabricated by a conventional photolithography technique, where GST memory devices were also fabricated for comparison. The set-reset switching behaviors of the devices were measured using a semiconductor parameter analyzer (Agilent 4155C) and a pulse generator (Agilent 33250A).

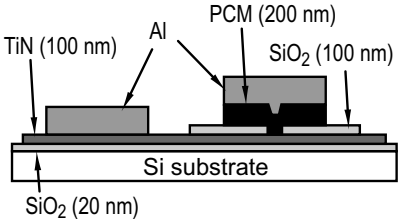

Figure 2 Schematic cross-sectional view of fabricated memory device.

To investigate the crystallization behaviors and thermal stability, GCT films were deposited on SiO_2(20 nm)/Si substrates by sputtering of GCT alloy target. The temperature and time dependences of the electrical resistance of films were investigated by in situ measurement with two-point probe method in Ar atmosphere. X-ray diffraction (XRD) analysis was performed for structural identification at room temperature. X-ray spectra were taken in the 2θ range of 20-60° using Cu-Kα with a scanning step of 0.02°. The film thickness change upon crystallization was evaluated by measuring the thickness of the film with an atomic force microscope (AFM) at room temperature. For the film thickness measurements, the films were heated up to different temperatures at a heating rate of 10°C/min and then cooled to room temperature. The film thickness was 200 nm for the two-point probe, XRD and AFM measurements. DSC measurements were also employed to investigate the thermal stability of GCT amorphous films. For this DSC measurement, GCT film with a thickness of 1500 nm were deposited on SiO_2(20 nm)/Si substrates in order to clearly detect an exothermic peak for crystallization.

3. RESULTS & DISCUSSION

3-1. Phase change temperatures and switching behaviors of GCT films

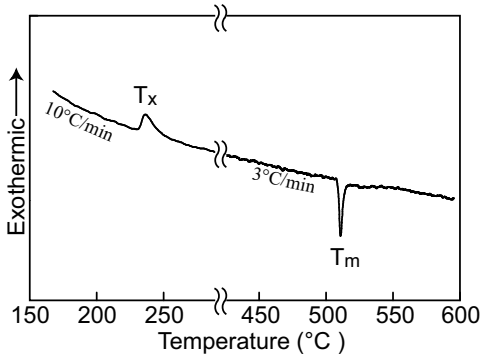

Figure 3 DSC curve of as-deposited GCT film, where crystallization temperature T_x and melting point T_m were measured at heating rates of 10°C/min and 3°C/min, respectively.

Figure 3 shows a DSC heating curve for the as-deposited GCT film. The crystallization temperature T_x was measured at a heating rate of 10°C/min and was detected to be about 235°C. The melting point T_m was determined to be 510°C at a heating rate of 3°C/min, which is in good agreement with the phase diagram as shown in Fig. 1. It is seen that GCT film shows a higher T_x and a lower T_m than GST film.

Figures 4(a) and (b) show the plots of device resistance vs. voltage applied to the device for the GCT and GST memory devices, respectively. It is seen from Fig. 4(a) that the GCT memory device shows set-reset switching behaviors as well as the GST memory device as shown in Fig. 4(b). In the present study, set voltage V_{set} and reset voltage V_{reset} were defined as the lowest voltages at which the electrical resistance change of over 10-fold is obtained for the set and reset operations, respectively. It is seen from Figs. 4(a) that the V_{set} and V_{reset} for the GCT memory device are 2.4 V and 5.7 V, respectively. Generally, since the power consumption for reset operation is much higher than that for set operation, the reduction of the power consumption for reset operation is much helpful to lower the net power consumption of PCRAM devices. The power consumption W_{reset} for the reset operation can be estimated by the relation of $(V_{reset})^2/R_{PCM}$, and the W_{reset} for the GCT and GST memory devices are estimated to be 0.55 W and 0.61 W, where the electrical resistance R_{PCM} was obtained by averaging the electrical resistance of the set state of the devices. The power consumption ratio $W_{reset}^{GCT/GST}$ of the GCT to GST memory devices is calculated to be 0.9, which means that the GCT memory device achieves a 10% reduction in power consumption for the reset operation compared with the GST memory device, which is mainly due to a lower melting point of GCT compound [13].

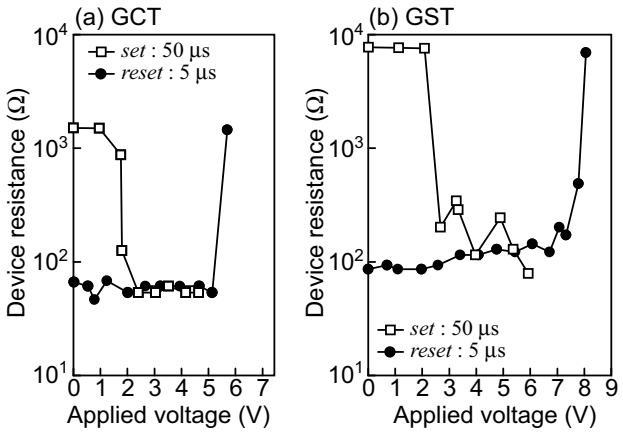

Figure 4 Set-reset switching behaviors of (a) GCT and (b) GST memory devices as a function of pulse voltage.

3-2. Crystallization behaviors

Figure 5 shows the temperature dependence of the electrical resistance of the GCT film at a heating rate of 60°C/min, where that of the GST film is also shown for comparison. The as-deposited GCT film was confirmed to be amorphous phase by the XRD pattern. It is seen that the GCT amorphous film has much lower electrical resistance and smaller temperature dependence of electrical resistance than the GST amorphous film. The GCT and GST films show a drastic resistance decrease of over 10^2-fold upon crystallization at about 260°C and about 180°C, respectively. After crystallization, the electrical resistance of the GCT film gradually decreases with further heating up to 400°C. Meanwhile, the GST film exhibits a step-like decrease at about 360°C, which is caused by the transition from an fcc to a hexagonal structure [3]. It is seen from Fig. 5 that the electrical resistance of the GCT crystalline phase hardly changes by cooling. And also, the electrical resistance of the GCT crystalline state is lower than that of the GST film. Figure 6 shows the XRD pattern obtained at room temperature from the GCT film heated up to 400°C followed by cooling to room temperature. It is seen from Fig. 6 that the GCT amorphous film crystallizes into a single $Ge_1Cu_2Te_3$ phase without phase separation, where Al peaks from sample holder are also observed. $Ge_1Cu_2Te_3$ phase is known to have an orthorhombic Imm2 structure [14].

Table 1 shows thickness change upon the crystallization of GCT and GST amorphous films, where the GCT and GST films were heated up to 300°C to crystallize into a $Ge_1Cu_2Te_3$ phase and a fcc phase, respectively. The GCT

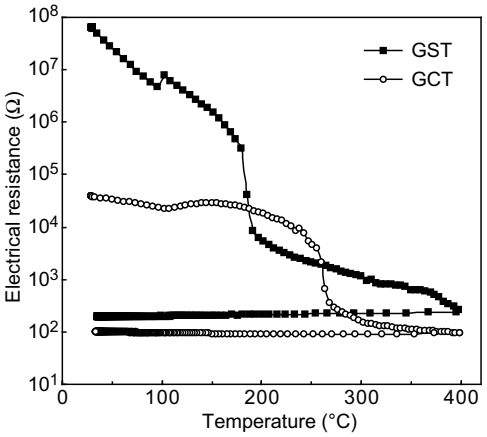

Figure 5 Temperature dependence of the electrical resistance of $Ge_1Cu_2Te_3$ (GCT) and $Ge_2Sb_2Te_5$ (GST) films.

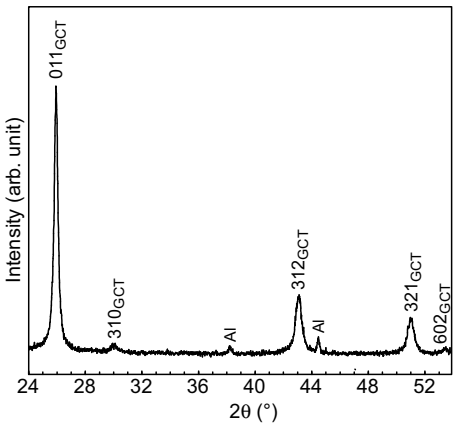

Figure 6 X-ray diffraction pattern of GCT film heated up to 400°C at heating rate of 10°C/min.

amorphous film shows a 2.0% thickness increase upon crystallization. Meanwhile the GST amorphous film shows a 6.0% decrease upon crystallization, which is in good agreement with the reported value of 6.5% [15]. It is seen from these results that the GCT film shows a smaller thickness change than the GST film, which means that the GCT film shows a smaller volume change than the GST film. Since the volume change induces stresses on the PCM as well as surrounding materials, it would limit the endurance of the devices [15]. Therefore, the GCT film with a small volume change is desirable to enhance the endurance of the PCRAM devices. Moreover, it is noteworthy that the changes are of opposite signs for the GCT and GST films. It has been reported that the bulk metallic glasses of $Pd_{40}Ni_{40-x}Cu_xP_{20}$ ($30 < x < 40$) expand upon crystallization since their crystalline phases have a relatively open structure and show a larger molar volume than their amorphous phases [16]. Therefore, it is suggested that the amorphous GCT possesses a smaller molar volume than the crystalline GCT.

Table 1 Film thickness change of the GCT and GST films upon crystallization.

	GCT [a]	GST [a]	GST [b]
Thickness change upon crystallization (%)	+ 2.0	- 6.0	- 6.5

a: present work
b: ref.[15]

3-3. Thermal stability of GCT amorphous film

The thermal stability of GCT amorphous films was evaluated by the time-dependent resistance change at different isothermal annealing temperatures. The thermal stability of the GST film was also evaluated for comparison. In this study, isothermal measurements were carried out at temperature ranging between 230°C and 245°C for the GCT film and at temperature ranging between 140°C and 155°C for the GST film. Figure 7 shows the time-dependent resistance change at 235°C, 239.5°C and 242°C for the GCT film. The electrical resistance decreases with crystallization and the onset time of the drastic decrease in the electric resistance becomes earlier with increasing the annealing temperature. The thermal stability of amorphous phase can be evaluated from Arrhenius plots of t_f vs. 1/T, where t_f is failure time and T is annealing temperature. Generally, the failure time t_f was defined as the time when the electrical resistance decreases by 10% of the initial value, $t_f^{10\%}$ [17] or as the time when the resistance decreases by a factor of two, $t_f^{50\%}$ [8] during annealing at a certain temperature. Figure 8 shows the Arrhenius plots for failure time $t_f^{10\%}$ and $t_f^{50\%}$ in the GCT and GST amorphous films. It is suggested from Fig. 8 that the GCT amorphous film shows 10-year data lifetime

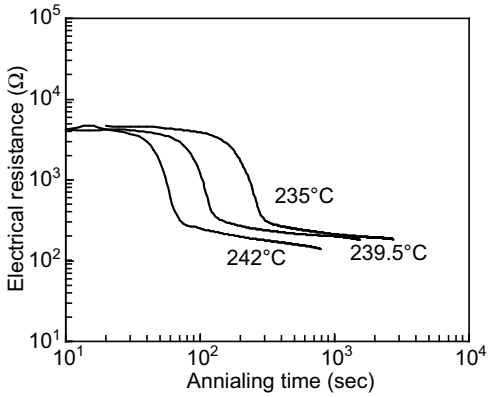

Figure 7 Time-dependent resistance change of GCT film at 235°C, 239.5°C and 242°C.

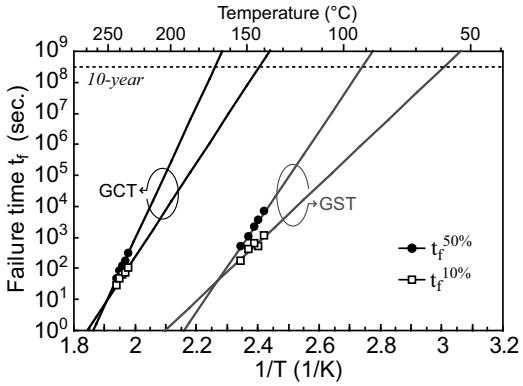

Figure 8 Arrhenius plots for the failure time $t_f^{10\%}$ and $t_f^{50\%}$ of the amorphous GCT and GST films.

at the maximum temperature of 143°C and 170°C for $t_f^{10\%}$ and $t_f^{50\%}$, respectively, while the GST amorphous film shows that of 59°C and 92°C for $t_f^{10\%}$ and $t_f^{50\%}$, respectively. These results imply that the amorphous GCT exhibits a higher thermal stability than the amorphous GST.

Although the two-point probe method under isothermal conditions is a simple method to evaluate the thermal stability of amorphous phases, the results can be affected by the heating rate at which the sample is heated up to a constant temperature. Meanwhile, the thermal stability of the amorphous phase at a given temperature can be estimated by kinetic parameters obtained under a non-isothermal condition. The time t_e to reach a crystallization fraction x at a given temperature T_i can be expressed as follows [18]:

$$t_e = \theta_n \exp\left(\frac{E_a}{RT_i}\right) \qquad (1),$$

where E_a is the activation energy of crystallization, and R is gas constant. θ_n is the reduced time proposed by Ozawa [18]. When the temperature is increased at a constant rate, θ_n is given by the following equation [19],

$$\theta_n = \frac{E_a}{\beta R} p\left(\frac{E_a}{RT_n}\right) \qquad (2).$$

Here, β is heating rate and T_n is temperature which yields a crystallization fraction x at a heating rate β. The p-function is approximately expressed as follows [19]:

$$\log p\left(\frac{E_a}{RT_n}\right) = -2.315 - 0.4567\left(\frac{E_a}{RT_n}\right) \qquad (3).$$

Equation (1) is generally applied to a single-step reaction with a constant activation energy. The temperature dependence of crystallization fraction x can be determined by DSC measurement. Figure 9(a) shows a portion of a DSC heating curve measured at a heating rate of 40ºC/min for the GCT film. An exothermic peak corresponding to crystallization appears in the temperature range of 245-265°C. As shown in Fig. 9(a), the crystallization fraction x at a temperature T is given by x=A_T/A, where A is the total area of the exothermic peak between the starting (T_s) and finishing (T_f) temperatures for the crystallization and A_T is the area between the T_s and T [20]. Figure 9(b) shows the crystallization fraction x as a function of temperature. In this estimation, failure time $t_e^{10\%}$ is defined as the time to reach a crystallization fraction of 10%. Figure 10 shows $t_e^{10\%}$ vs. T_i curves of the GCT and GST films. For the GCT film, the values used for the calculation of the $t_e^{10\%}$ are β = 40°C/min, T_n = 248.6°C which is obtained from Fig. 9(b)

and E_a = 2.81 eV which was obtained from Kissinger plots using the results of two-point probe resistance measurements [11]. It should be noted that the calculated result is not dependent on the heating rate. For the GST film, the $t_e^{10\%}$ was calculated using T_n = 155°C obtained from a DSC curve at β = 10°C/min and E_a = 2.87 eV in the literature [17]. From the Ozawa method, the maximum temperature for 10-year data lifetime can be estimated to be 135°C and 80°C for the GCT and GST films, respectively. Although these estimated values are lower than the valued obtained from the isothermal measurements, the thermal stability of the GCT film is still well beyond the data retention requirement of ITRS.

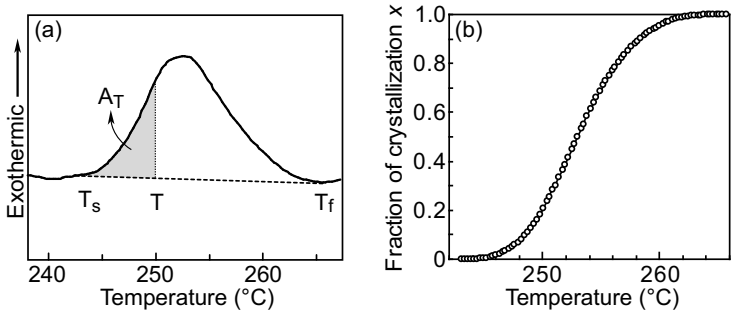

Figure 9 (a) DSC heating curve of the GCT film obtained at heating rate of 40°C/min. (b) Plots of Crystallization fraction *x* as a function of temperature obtained from the DSC curve.

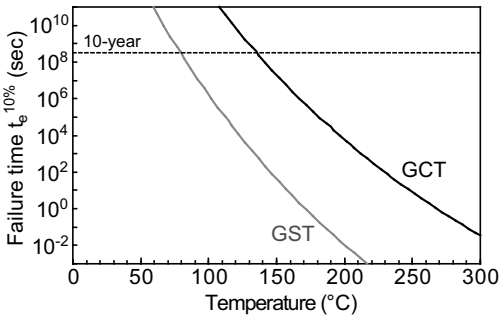

Figure 10 Temperature dependence of failure time $t_e^{10\%}$ for the GCT and GST films.

4. CONCLUSION

The as-deposited GCT film was found to show a high crystallization temperature of about 235ºC and a low melting point of about 510ºC by the DSC measurement. Moreover, it was confirmed that the GCT film shows a reversible phase transition and the GCT memory device has a 10% lower power consumption for reset operation than the GST memory device. Since the amorphous GCT has a high thermal stability and crystallizes to a stable single crystalline phase and shows a small volume change upon crystallization, the GCT devices are expected to show good data retention and endurance. Therefore, the GCT film can be expected to be a promising PCM for PCRAM application.

Acknowledgments

This work was supported by "Japan Science and Technology Agency" and KAKENHI (23360297).

REFERENCES

[1] N. Yamada, E. Ohno, K. Nishiuchi, N. Akahira and M. Takao, J. Appl. Phys. 69, 2849 (1991).

[2] S. Lai, T. Lowrey, IEDM Tech. Dig. 36.5.1 (2001).

[3] I. Friedrich, V. Weidenhof, W. Njoroge, P. Franz, M. Wuttig, J. Appl. Phys. 87, 4130 (2000).

[4] N. Ohshima, J. Appl. Phys. 79, 8357 (1996).

[5] T.H. Jeong, M.R. Kim, H. Seo, S.J. Kim, S.Y. Kim, J. Appl. Phys. 86, 774 (1999).

[6] J. González-Hernández, E.F. Prokhorov, Y.V. Vorobiev, J. Vac. Sci. Technol. A 18, 1694 (2000).

[7] B. Laine, C. Rivera-Rodrígues, E. Morales-Sánchez, E. Prokhorov, G. Trapaga, J. González-Hernández, J. Non-Cryst. Solids 345&346, 173 (2004).

[8] A.L. Lacaita, Sol. State. Electro. 50, 24 (2006).

[9] A. Redaelli, D. Ielmini, U. Russo, A.L. Lacaita, IEEE Trans. Electro. Dev. 53, 3040 (2006).

[10] B. Gleixner, A. Pirovano, J. Sarkar, F. Ottogalli, E. Tortorelli, M. Tosi, R. Bez, Proc. IRPS Tech. Dig. 2007, p. 542.

[11] Y. Sutou, T. Kamada, Y. Saito, M. Sumiya and J. Koike, Mater. Res. Soc. Symp. Proc. 1251, H05-08 (2010).

[12] M. Dogguy, C. Carcaly, J. Rivet et Jean Flahaut, J. Less-Common Metals 51 (1977) 181.

[13] T. Kamada, Y. Sutou, Y. Saito, M. Sumiya and J. Koike, to be submitted.

[14] G.E. Delgado, A.J. Mora, M. Pirela, A.V. Velasquez, M. Villarreal, B.J. Fernandez, Phys. Stat. Sol. (a) 201, 2900 (2004).

[15] T.P. Leervad Pedersen, J. Kalb, W.K. Njoroge, D. Wamwangi, M. Wuttig, Appl. Phys. Lett. 79, 3597 (2001).

[16] T.D. Shen, U. Harms, R.B. Schwarz, Appl. Phys. Lett. 83, 4512 (2003).

[17] T. Zhang, Z. Song, F. Wang, B. Liu, S. Feng, B. Chen, Jpn. J. Appl. Phys. 46, L602 (2007).

[18] T. Ozawa, Bull. Chem. Soc. Jpn. 38, 1881 (1965).

[19] T. Ozawa, J. Therm. Anal. 2, 301 (1970).

[20] D.W. Henderson, J. Non-Cryst. Solids **30**, 301 (1979).

Biographies

Y. Sutou studied materials science at Tohoku University and received his PhD at the same University in 2001. He is an associate professor of the device reliability science and engineering at Department of Materials Science, Graduate School of Engineering, Tohoku University. His research field is material design and microstructure control of shape memory alloys, phase change memory materials, interconnects for semiconductor, hard coating etc.